Journal of Inorganic Biochemistry 195 (2019) 164–173

Contents lists available at ScienceDirect

Journal of Inorganic Biochemistry

journal homepage: www.elsevier.com/locate/jinorgbio

Mannich base Cu(II) complexes as biomimetic oxidative catalyst

Bidyut Kumar Kundu[a], Rishi Ranjan[a], Attreyee Mukherjee[b], Shaikh M. Mobin[a], Suman Mukhopadhyay[a,c,*]

[a] Discipline of Chemistry, School of Basic Sciences, Indian Institute of Technology Indore, Khandwa Road, Simrol, Indore 453552, India
[b] Department of Chemistry, Ananda Mohan College, Kolkata 700009, India
[c] Discipline of Biosciences and Biomedical Engineering, School of Engineering, Indian Institute of Technology Indore, Khandwa Road, Simrol, Indore 453552, India

A B S T R A C T

Galactose Oxidase (GOase) and catechol oxidase (COase) are the metalloenzymes of copper having monomeric and dimeric sites of coordination, respectively. This paper summarizes the results of our studies on the structural, spectral and catalytic properties of new mononuclear copper (II) complexes [CuL(OAc)] (**1**), and [CuL_2] (**2**), (HL = 2,4-dichloro-6-{[(2′-dimethyl-aminoethyl)methylamino]methyl}-phenol) which can mimic the functionalities of the metalloenzymes GOase and COase. The structure of the compounds has been elucidated by X-ray crystallography and the mimicked Cu(II) catalysts were further characterized by EPR. These mimicked models were used for GOase and COase catalysis. The GOase catalytic results were identified by GC–MS and, analyzed by HPLC at room temperature. The conversion of benzyl alcohol to benzaldehyde were significant in presence of a strong base, Bu_4NOMe in comparison to the neutral medium. Apart from that, despite of being monomeric in nature, both the homogeneous catalysts are very prone to participate in COase mimicking oxidation reaction. Nevertheless, during COase catalysis, complex **1** was found to convert 3,5-ditertarybutyl catechol (3,5-DTBC) to 3,5-ditertarybutyl quinone (3,5-DTBQ) having greater rate constant, k_{cat} or turn over number (TON) value over complex **2**. The generation of reactive intermediates during COase catalysis were accounted by electrospray ionization mass spectrometry (ESI-MS). Through mechanistic approach, we found that H_2O_2 is the byproduct for both the GOase and COase catalysis, thus, confirming the generation of reactive oxygen species during catalysis. Notably, complex **1** having mono-ligand coordinating atmosphere has superior catalytic activity for both cases in comparison to complex **2**, that is having di-ligand environment.

1. Introduction

Enzymatic reactions have motivated a lot of researchers to plan some small molecule imitates which can perform the function of the enzymes under various catalytic conditions [1,2]. Among which metalloenzymes is a class of efficient biological catalysts showing high catalytic conversion of organic substrates where metal ion cofactor attached to the amino acids side chain in its active site(s) plays the most crucial role [3]. Copper having significant redox properties can be found in many metalloenzyme, which allows it to participate in various oxidation reactions [4,5]. Cu(II) containing metalloenzymes are basically surrounded by the coordinate-covalent bonds with −N/−O donor centers mostly from the side chains of amino acids [5]. However, mimicking structural and functional properties of any metalloenzyme, by synthesized transition metal coordination complexes, is of great interest for past few decades [6,7]. Yet, complicated synthetic procedures of suitable mimics, stability in homogeneous conditions, lower solubility of catalysts in organic or aqueous-buffer media, less conversion efficiency of catalytic substrates, and extreme reaction conditions are the prominent challenges, which need to be explored for further improvement.

Galactose Oxidase (GOase) is a mononuclear type II copper fungal metalloenzyme, which is efficient for two e^- transfer oxidation of primary alcohols to aldehydes [8–10]. Its active site consists of two oxygen atom of tyrosine (Tyr272 and Tyr495) and two nitrogen atom of histidine (His496 and His581) protein residues to coordinate with Cu (II) center along with a labile water molecule (pH ~ 7) to form a distorted square pyramidal geometry as depicted in Scheme 1 [11,12]. Sometimes water can be replaced by an acetate group at lower pH ~ 3.5. Furthermore, this enzyme is capable of dioxygen reduction to hydrogen peroxide under aerobic condition [2,13]. Therefore, to activate aerial oxygen by using laboratory synthesized transition metal complexes is an important phenomena towards green oxidation based on bio-inspired perception. Furthermore the importance of oxidation of primary alcohol into aldehyde lies in the fact that aromatic aldehydes are widely used for a flavor in chocolates, chewing gums, and ice creams, etc. [14,15] Moreover, these can be easily oxidized to acids, which have appreciable water solubility, and can act as a preservative in many drinks [16]. The design of N_2O_2 based mononuclear Cu(II) based GOase enzyme is thus too important to understand to follow the mechanistic pathways of original enzyme. Hence, researchers have focused to the synthesis of salen based ligand (N_2O_2), or N_3O model as

* Corresponding author at: Discipline of Chemistry, School of Basic Sciences, Indian Institute of Technology Indore, Khandwa Road, Simrol, Indore 453552, India.
E-mail address: suman@iiti.ac.in (S. Mukhopadhyay).

https://doi.org/10.1016/j.jinorgbio.2019.03.023
Received 22 January 2019; Received in revised form 23 March 2019; Accepted 28 March 2019
Available online 30 March 2019
0162-0134/

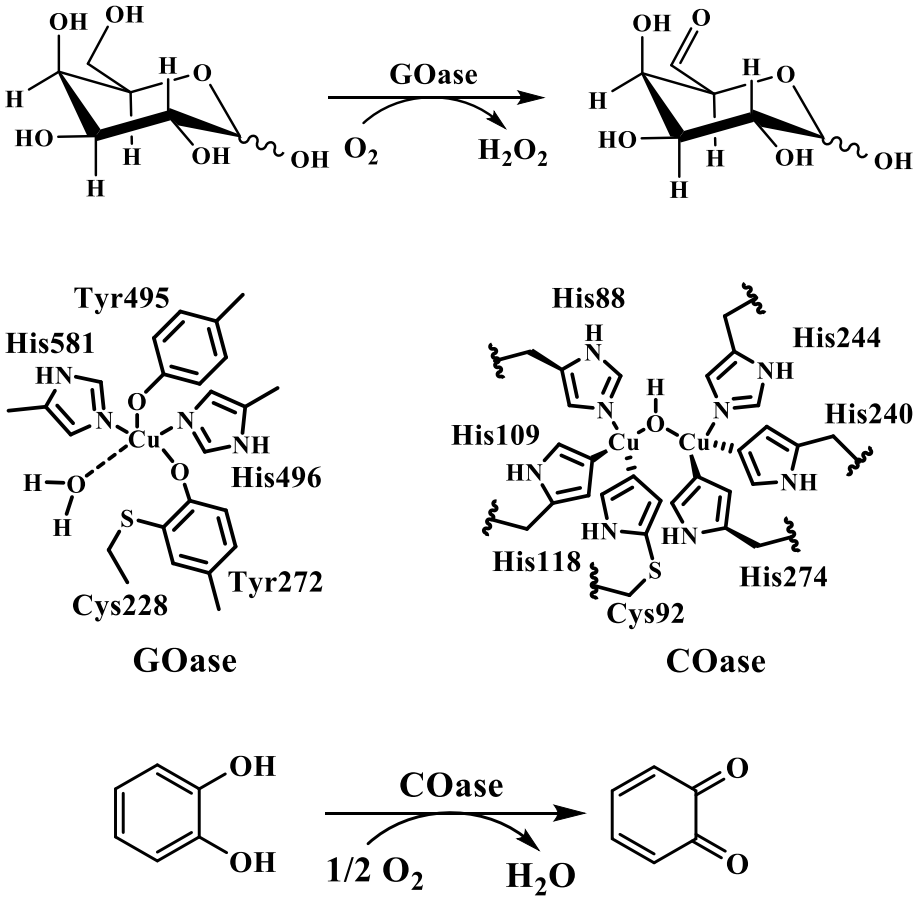

Scheme 1. Structural and functional model of galactose oxidase (GOase), and catechol oxidase (COase).

GOase analogues in recent past [17–19]. Despite of being functionally similar, the mechanistic approach of GOase catalysis needs to be explored further for better understanding and improved activity.

Apart from that, as described in Scheme 1, catechol oxidase (COase) is a type III di-copper plant or fungi cofactor surrounded by six histidine residues [20–22]. This is well known for the reversible binding of molecular oxygen at ambient conditions. It oxidizes ortho di-phenols into ortho quinones along with reduction of O_2 to H_2O [23]. Ripening of fruits or vegetables is the primary cause of quinone formation by COase catalyst [24,25]. The production of quinone based compounds can be used to generate potent anticancer agents, scavenging agent of sulphides, mercaptans, and cyanides, and can inhibit proteases or bone marrow function. However, there are numerous reports on the several transition metals based small molecule organic mimics of COase, but many of those are either less active towards catalysis, or lack of mechanistic evidence [26–29].

Although, lots of Schiff base complexes based on −N/−O donors have been synthesized over the years to mimic the functional properties of metalloenzymes [30–32] but the stability of them are always in question in fully aqueous-buffer media as the imine double bond is prone to hydrolysis. In comparison to Schiff base, which is capable of electrophilic substitution for its imine bond, Mannich base compounds which are not easily hydrolysable in aqueous and non-aqueous solvents are more potent candidates. In spite of lower conversion efficiency with respect to original enzyme, laboratory synthesized catalysts can show more susceptibility towards higher temperature, and large solvent scope.

Herein, we have synthesized two mononuclear Cu(II) Mannich base complexes to check the galactose oxidase (GOase) and catechol oxidase (COase) mimicking activity. Complex CuL(OAc) (**1**) [HL = 2,4-dichloro-6-{[(2′--dimethyl aminoethyl)methylamino] methyl}-phenol] with N_2O_2 site of coordination can act as proper GOase and COase mimics. Moreover, a di-ligand based octahedral complex [CuL_2] (**2**) have been also been synthesized to compare the catalytic activity with that of **1**.

2. Experimental section

Kindly consult to the electronic supplementary for the details instrumentation.

2.1. HPLC analysis to monitor GOase mimicking activity

The method for recording high performance liquid chromatography (HPLC) was taken as described earlier [33]. Kindly consult to the supporting information for the details elaboration.

2.2. Synthesis and characterization

2.2.1. Synthesis of 2,4-dichloro-6-{[(2′-dimethyl aminoethyl) methylamino]methyl}-phenol, (HL)

An improved synthetic method has been applied for synthesizing the novel Mannich base ligand, **HL** [34]. The detailed synthetic procedure is described in Section S05 of ESI†.

2.2.2. Synthesis of 2,4-dichloro-6-{[(2′-dimethylaminoethyl)methylamino] methyl}-phenolcupric acetate, CuL(OAc) (1)

A solution of **HL** (0.14 g; 0.5 mmol), triethylamine (76 μL; 0.5 mmol), and $Cu(OAc)_2$. H_2O (0.1 g; 0.5 mmol) in MeOH (15 mL) was stirred under refluxing for 4 h. The dark greenish microcrystalline solid was collected by filtration. Several methods have been employed to obtain single crystals of the compound. However, in almost all cases the

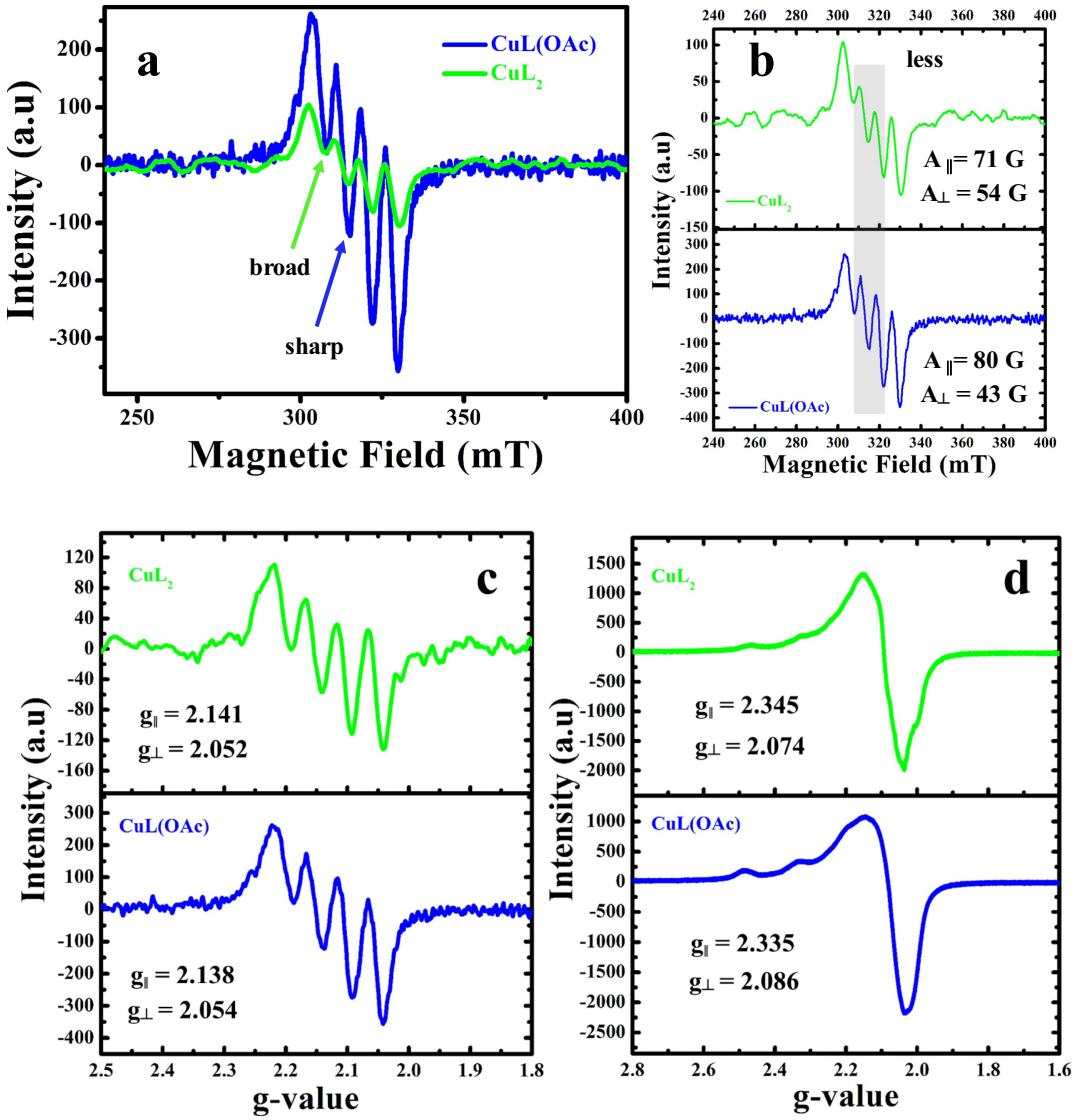

Fig. 1. (a) to (c) represents the EPR spectra of homogeneous catalysts at room temperature in CH_2Cl_2; where, (a) merged plot of the complexes **1** and **2**, (b) stacking diagram showing noisy peaks of complex **2**, (c) 'g' parameters of **1** and **2**, and (d) solid phase EPR spectra of **1** and **2** and their corresponding 'g' values at 77 K.

diffraction pattern in very weak and remains non-reportable. Yield: 0.204 g (~86%). Anal. Calcd (%) for $C_{14}H_{20}Cl_2CuN_2O_3$: C, 42.17; H, 5.06; N, 7.02; Found (%): C, 42.20; H, 5.08; N, 6.98; FTIR (in KBr, υ in cm^{-1}): 1663, 1460 {$\upsilon_{C=O,}$ (**s**)}; 3640–3610 {$\upsilon_{C\text{-}O,}$ (s, sh)}; 3000–2850 {$\upsilon_{C\text{-}H,}$ (m)}; 1250–1020 {$\upsilon_{C\text{-}N,}$ (m)} (Fig. S2). ESI-MS in HPLC MeOH (+, *m/z*): $\{C_{14}H_{20}Cl_2CuN_2O_3\}^+$: 399.8(100%), $\{C_{14}H_{20}Cl_2CuN_2O\}^+$: 340.0 (Fig. S3b); UV–Vis in HPLC MeOH: (λ_{max}, nm): 440.

2.2.3. Synthesis of bis-[2,4-dichloro-6-{[(2′-dimethylaminoethyl) methylamino]methyl}-phenol] cuprate, CuL_2 (2)

Complex **2** have also been synthesized as described above. The respective ligand (0.27 g; 1.0 mmol), was dissolved in 20 mL of MeOH followed by addition of triethylamine (152 μL; 1.0 mmol) and Cu $(OAc)_2$. H_2O (0.1 g; 0.5 mmol). The formation of the complex was immediately indicated by a change in colour. After stirring the mixture for 3 h at room temperature, the mixture was filtered through a filter paper and the solvent was removed in vacuo. Crystals suitable for X-ray diffraction analysis were obtained through slow vapour diffusion process by di-iso-propyl ether into CH_2Cl_2-CH_3CN (1:1) mixture of complex. Yield: 0.342 g (~91%). Anal. Calcd (%) for $C_{24}H_{34}Cl_4CuN_4O_2$: C, 46.80; H, 5.56; N, 9.10; Found (%): C, 46.76; H, 5.61; N, 9.15; FTIR (KBr υ in cm^{-1}): 3100–3000 {$\upsilon_{C\text{-}H,}$ (s); 3000–2850 {$\upsilon_{C\text{-}H,}$ (m)},1580–1459 {$\upsilon_{C\text{-}C,}$ (s)}; 1250–1020 {$\upsilon_{C\text{-}N,}$ (m)} (Fig. S2). ESI-MS in HPLC MeOH (+, *m/z*): $\{C_{24}H_{34}Cl_4CuN_4O_2\}^+$: 616.1(100%) (Fig. S3c); UV–Vis in HPLC MeOH: (λ_{max}, nm): 444.

Where, the above abbreviations define; (s) = strong; (m) = medium, and (sh) = sharp band.

3. Results and discussion

3.1. Synthesis of compounds

Both the compounds were isolated as solid crystalline form (Scheme S1). Ligand and its complexes have been characterized by several analytical techniques viz. ^1H, and ^{13}C NMR, FTIR, electrospray ionization mass spectrometry (ESI-MS), thermogravimetric analysis (TGA), and cyclic voltammetry (CV). To obtain different metal complexes ligand to metal ratio have been varied. Apart from the reported NMR peaks, the molecular ion peak of ligand appears at 277.1, followed by the formation of stable iminium ion with mass of 115.1 in the first step of Mannich reaction. Complex **1** has shown molecular ion peak at 399.8, whereas that of complex **2** is 616.1. An additional peak at 340.0 in complex **1** comes for the easily dissociable labile acetate group to form stable $[CuL]^+$. FTIR spectrum of complex **1** indicates the

stretching frequencies at 1663, 1460 cm^{-1} due to the asymmetric and symmetric stretching of acetate group [35], which is absent in the complex **2**. Complex **2** possesses some common weak bands in the range of 1250–1020 cm^{-1} assigned for $\upsilon_{C\text{-}N}$ bond [36]. Thermogravimetry profile suggests that 58.2% weight loss is happening for the release of iminium moiety at 228 °C for **HL** (Fig. S4). Moreover, complex **2** is more stable than that of complex **1** and both showing considerable first degradation around 246 °C. Furthermore, wavelength maxima obtained at 445 and 439 nm for complex **1** and **2** is responsible for the metal-to-ligand charge transfer (MLCT) transition [37].

The electrochemical behaviour of the Mannich base phenolic ligand and its complexes were investigated by cyclic voltammetry analysis using Bu_4NPF_6 as the supporting electrolyte in dichloromethane. The redox potentials are quoted against Ag^+/AgCl electrode couple (Fig. S5, Table S1). Upon oxidation of **HL**, an anodic peak at $E_{pa} = +0.86$ V was observed along with a highest cathodic peak, $E_{pa} = +0.71$ V providing quasi-reversible behaviour of phenoxyl moiety [38,39]. Quasi-reversible peaks are also observed for complexes **1** and **2** for metal centered redox behaviour whereas ligand centered peaks become less prominent. Oxidation potential ranges of complexes **1** and **2** from +0.89 to +1.20 V suggest that it requires an external oxidant for oxidation process [40]. Moreover, the solution and solid state electron paramagnetic resonance (EPR) spectra of both the copper complexes were recorded at 298 K and 77 K, respectively. Both the $A_{\parallel}$ and $g_{\perp}$ values of complex **1** is greater than that of complex **2** (Fig. 1). A less intense noisy spectra was observer for **2** having larger $A_{\perp}$ and $g_{\parallel}$ values ($A_{\perp} = 54$ gauss, and $g_{\parallel} = 2.141$). As depicted in Fig. 1, the solid phase EPR signals at liquid nitrogen temperature having $g_{\perp}$ at 2.086, and $g_{\parallel}$ at 2.335 for complex **1**, respectively, ascribed to the unpaired electron of Cu^{II} (d^9 system), results in a paramagnetic system. Similarly, $g_{\perp}$ at 2.074 and $g_{\parallel}$ at 2.345 in case of complex **2** signifies the paramagnetic nature of distorted octahedral geometry [41].

3.2. Single crystal X-ray diffraction study (XRD)

Ligand, **HL** and complex **2** have been characterized by X-ray crystallography. These two compounds are monoclinic in nature having space group of P 21/c. Fig. 2 represents the ORTEP diagram of **HL** and complex **2** having 50% thermal probability of ellipsoids. The structure refinement parameters are summarized in Table S2 and the selective bond angles and bond lengths are presented in Table S3. There is a prominent intramolecular hydrogen bond in ligand HL between O1—H101…N2 (Fig. S6). There are two crystallographically independent copper ions and both of them show octahedrally coordinated geometry which are fulfilled by four N atom of ligand and two phenoxide O atom. Two molecules of complex **2** may interact with each other via. C—H…π (C23 of Cu(2) and centroid of Cu(1)) force of attraction (Fig. S6). Those molecules also form intermolecular hydrogen bond between Cl(1)…H(17)—C, which can be further extended to form a 1D or 2D polymeric sheet (Fig. 2c) [42,43]. There are not many non-covalent interactions observed between the individual molecules. All the bond lengths and angles are in good agreement with earlier reports [23,36]. Furthermore, geometry optimized structure of complex **1** was elucidated by density functional theory (DFT) (using similar basis set as used in our previous reports [37,44]), and the corresponding structure along with bond lengths and bond angles around the central metal is depicted in Fig. S7.

3.3. Galactose oxidase (GOase) catalysis

3.3.1. Galactose oxidase mimicked aerial oxidation of benzyl alcohol

A 2.5×10^{-4} M solution of complexes used as GOase mimicked catalyst to oxidize substituted benzyl alcohol (substrate concentration range of $10 \times 10^{-3} - 2.5 \times 10^{-1}$ M) in CH_2Cl_2. 0.8 equivalent tetrabutylammonium methoxide, n-Bu_4NOMe (TBAM) was added at the initial stage of catalysis to abstract primary alcoholic proton. After that, the whole mixture was stirred at room temperature in air. The solution was diluted as required for acquisition of the electronic spectra using a blank with the catalyst as well as standard substrates. HPLC and gas chromatography (GC) were performed for quantitative determination of the concentration of major oxidized product.

Caution! *The solvents used for this catalysis should be free from any aliphatic or aromatic primary −OH functional group.*

3.3.2. Change in electronic spectra during GOase catalysis

Benzyl alcohol has been taken as a substrate for alcohol oxidation, with a λ_{max} (wavelength maxima) of 256 nm ($\pi \rightarrow \pi^*$ transition) [37]. In CH_2Cl_2 solution, the mononuclear complex **1** gives a strong d-d band at 685 nm having molar extinction coefficient (ε in $Lmol^{-1}\,cm^{-1}$) of 4.9×10^2 (inset representation of Fig. 3a). As describes above, the catalytic mixture was subjected to perform UV–Vis analysis after 5 h of interval. The generation of a new peak at 290 nm is assigned to the formation of benzaldehyde as oxidized product, which was further confirmed by a blank experiment (inset plot of Fig. 3a). It shows that optical density at 290 nm, responsible for the oxidized product is greater for catalyst **1** with respect to catalyst **2**, signifying the better catalytic activity of complex **1** (Fig. 3a). Fig. 3b is the representation of time dependent catalysis by most active catalyst **1**. Absorbance at 290 nm increases with increasing the duration of catalysis, which was further plotted as shown in the inset (a) of Fig. 3b. A plot of molar extinction coefficient is shown in Fig. S8a, resulting a nonlinear fitted saturated equilibrium curve after 20 h of catalysis (Table S4).

3.3.3. Monitoring the oxidation of substituted benzyl alcohol

Room temperature catalytic oxidation of benzyl alcohol to benzaldehyde and/or benzoic acid were monitored by taking 0.125 M of each substrate in 10 mL of dichloromethane by fixing the catalyst concentration of 2.5×10^{-3} M. The results were analyzed via HPLC analysis at the wavelength maximum of 254 nm and 290 nm, respectively. One equivalent of strong base, tetrabutylammonium methoxide (TBAM) has been used in each oxidation reaction because alcoholic proton does not get easily dissociated in presence of a weak base. As summarized in Table 1, benzyl alcohol gets converted of 93.43% and 92.80% in 8 h by using catalyst **1** and **2**, respectively to produce benzaldehyde as sole product. This oxidized product is 100% selective. A percentage conversion up to 3–5% have increased within 12 h of catalysis.

Although, we varied a series of substrate to get the proper substitutional effect, but these are not following the regular trends depending upon the electronic properties of the functional group attached to the benzyl alcohol. However, chloro-substituted benzyl alcohol has been found to show better conversion rate with respect to bromo substitution. This might be attributed to the greater electron withdrawing effect of chloro group over bromo. Moreover, electron donating methyl and isopropyl-substituted substrates also provide a high percentage conversion within 12 h.

Fig. 4 represents the product(s) formed after catalysis in 8 h. Pure references of substrate and product were taken to get the value of retention time before analysing the catalytic mixture. Apart from producing aldehydes, substituted benzyl alcohols have also given the corresponding benzoic acid. Furthermore, the selectivity of benzaldehyde decreases with increase in time. Apart from that, variation in the amount of base is directly related to the percent conversion of oxidized products. As shown in Fig. S8, upon increasing the amount of base increment in the percentage conversion has been observed. This reaches to maximum (42.26% within 3.5 h) when the ratio of substrate: base is 1:1 (Table S5). Although 0.8 equivalent of base is very effective to covert 41.93% in 3.5 h. Hence, it seems that one equivalent of base is required to abstract one proton of primary aryl alcohols. Furthermore, a table having competitive kinetic parameters on GOase catalysis have been summarized in Table S6, which shows that the complex **1** is having greater K_{cat} value of $2.8 \times 10^{-3}\,s^{-1}$ over complex **2** having

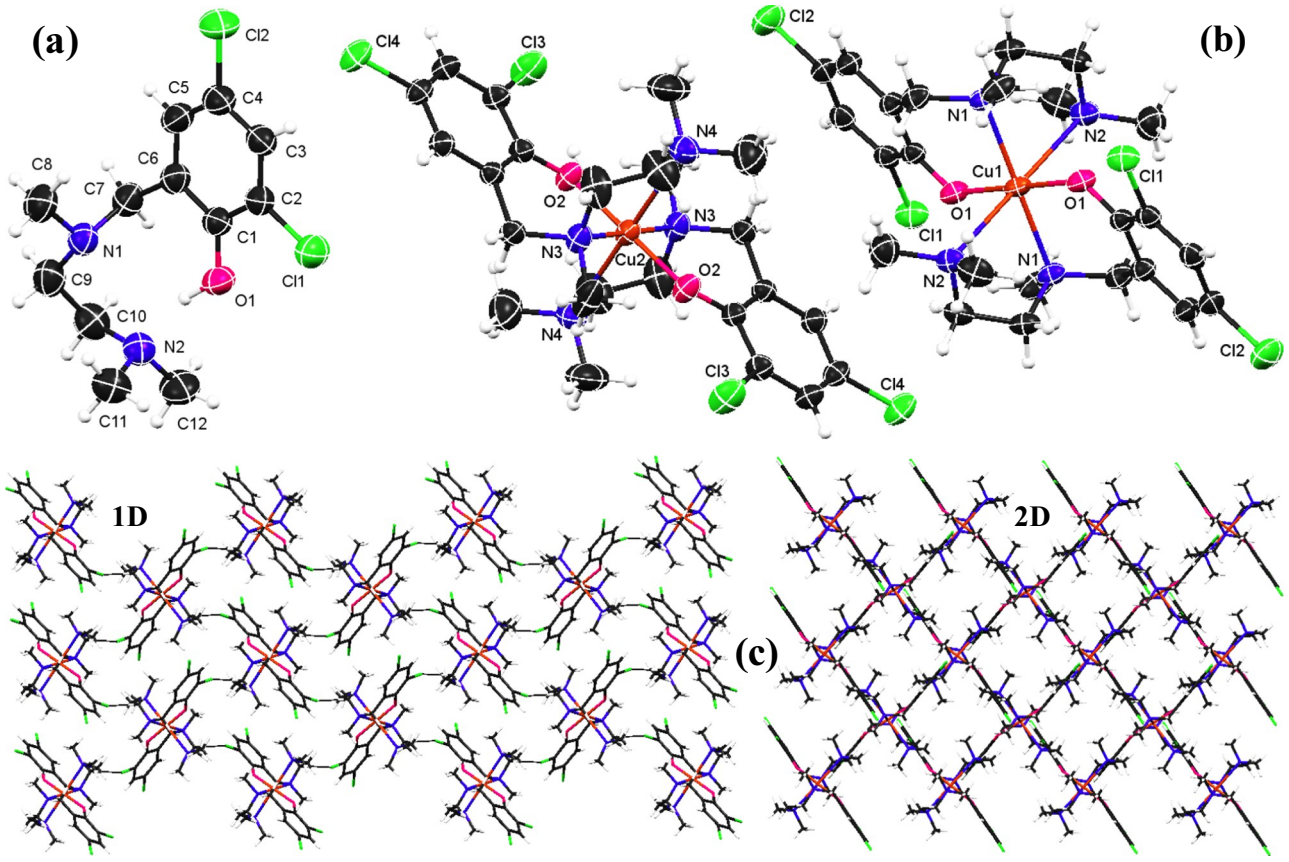

Fig. 2. ORTEP view with 50% probability of ellipsoids showing geometric displacement and partial atomic labels for (a) **HL**, (b) **CuL_2**, and (c) polymeric extension through intermolecular H-bonding.

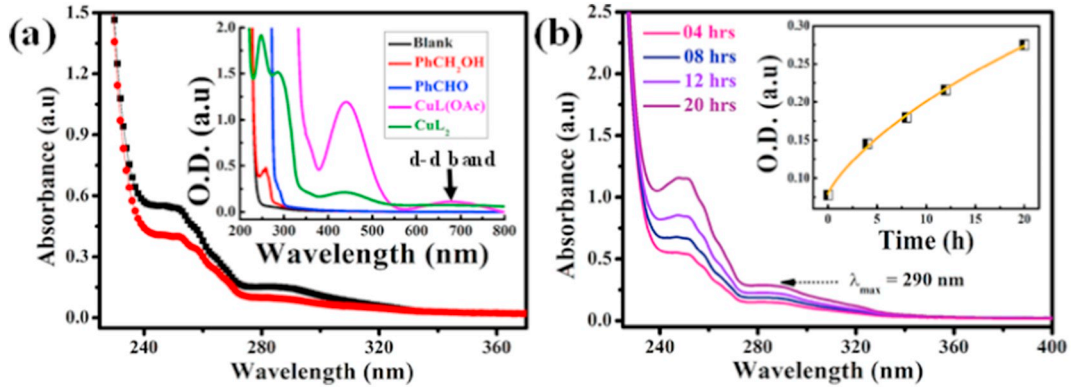

Fig. 3. Electronic spectra of the complexes and the catalytic mixture in CH_2Cl_2 at 25 °C: (a) Changes in the UV–Vis spectrum during the course for reaction with benzyl alcohol (0.4 M) by complex **1** and **2** (2.5×10^{-4} M), in 5 h (colour significance: black = catalysis by CuL(OAc), red = catalysis by CuL_2, inset: absorption profile of reference samples). (b) Gradual increment in O.D. value during benzyl alcohol oxidation by catalyst **1** (0–20 h, absorbance vs. time profile is on the inset plot). (For interpretation of the references to colour in this figure legend, the reader is referred to the web version of this article.)

same of $4.2 \times 10^{-4}\,s^{-1}$.

3.3.4. Mechanism of action for GOase like activity

Y. Wang et al. [40] elaborated the formation of active catalyst under 1 atm of O_2 (Scheme 2). Later on, the proposed mechanism of GOase mimicked was theoretically investigated by F. Himo et al. [45] According to that mechanism of original enzyme, it is presumed that substrate must be binding the metal center replacing the exogenous water or acetate in the equatorial position (Schemes 1 and 2). Although both the homogeneous catalysts contributed for the significant conversion, yet, we have chosen the catalyst **1** to describe the probable GOase like mechanism, as it contains one easily removable acetate group in its coordination sphere. In the very first step of this catalysis proton abstraction happens for the primary alcohol in presence of a strong base, though in original enzyme it is presumed that the axial tyrosine ligand is involved in proton abstraction. In the second step, the deprotonated form of the substrate prefers for a nucleophilic attack to the copper center by displacing labile acetate moiety attached to copper center (Scheme 2 and Scheme S2). Next step is regarding the hydrogen atom transfer from substrate to the phenolic O-atom. Generating a radical intermediate to favour the electron transfer from substrate to the metal center with a decrease its oxidation state from Cu(II) → Cu(I), with the concomitant generation of the oxidized product (i.e.; aldehyde). Moreover, the intermediate Cu(I) complex is very unstable and

Table 1
Percentage conversion of substituted benzyl alcohol by homogeneous catalysts **1** and **2**.

Entry	Substrates to check GOase activity	Time (h)	Conversion (%)		Time (h)	Conversion (%)	
			1	2		1	2
01		**08**	**93.43**	**92.80**	**12**	**98.56**	**95.34**
02	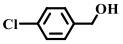	08	90.14	84.38	16	94.39	92.00
03	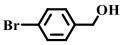	12	64.11	68.39	20	84.55	70.20
04	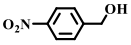	08	66.83	62.63	16	78.29	76.35
05	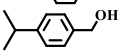	08	65.68	63.42	12	85.72	81.56
06	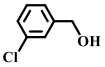	08	86.71	79.09	12	93.45	91.30
07	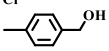	12	62.7	66.78	20	71.34	70.53

subjected to get back its oxidized form with the reduction of aerial oxygen producing hydrogen peroxide (H_2O_2) in the medium in the process.

3.4. Catecholase activity (COase) studies

3.4.1. Catechol oxidase mimicked aerial oxidation of 3,5-DTBC

3,5-Di-tert-butylcatechol (3,5-DTBC) has taken as the substrate to explore the COase like activity of the synthesized Cu(II) complexes. It is already reported that any kind of ortho diol can act as the substrate for the COase mimicking activity [46]. Moreover, the bulkiness of t-butyl substituents in the ring helps to decrease the reduction potential of catechol [1]. The working concentration range of 3,5-DTBC have been prepared from 50×10^{-4} M to 350×10^{-4} M upon fixing the catalyst strength of 4.0×10^{-4} M in methanol solvent. The time dependent oxidation reaction was monitored later on by UV–Vis spectroscopy at 25 °C. The standard solution of 3,5-DTBC, and 3,5-ditertarybutyl quinone (3,5-DTBQ) shows the absorption band maxima at 350 nm, and 400 nm, respectively. The rapid oxidation of 3,5-DTBC with respect to time, generates a new band at 400 nm. This is due to the formation of the oxidized product, 3,5-DTBQ (Fig. S10) [23]. Furthermore, the slope values of each concentration dependent experiment were evaluated by using kinetic software of UV–Vis spectrometer.

To understand the kinetic aspect of COase catalysis, the rate constant for a catalyst was determined by plotting the observed rates (slope values) vs. substrate concentrations. The data were interpreted by utilizing the Michaelis–Menten equation of enzyme kinetic [47]. Further, the linearization of Lineweaver – Burk plots gives the value of Michaelis – Menten constant (K_m) and maximum initial rate (V_{max}) (Fig. S11) [48]. The turnover number (TON or k_{cat}) of catalysts were

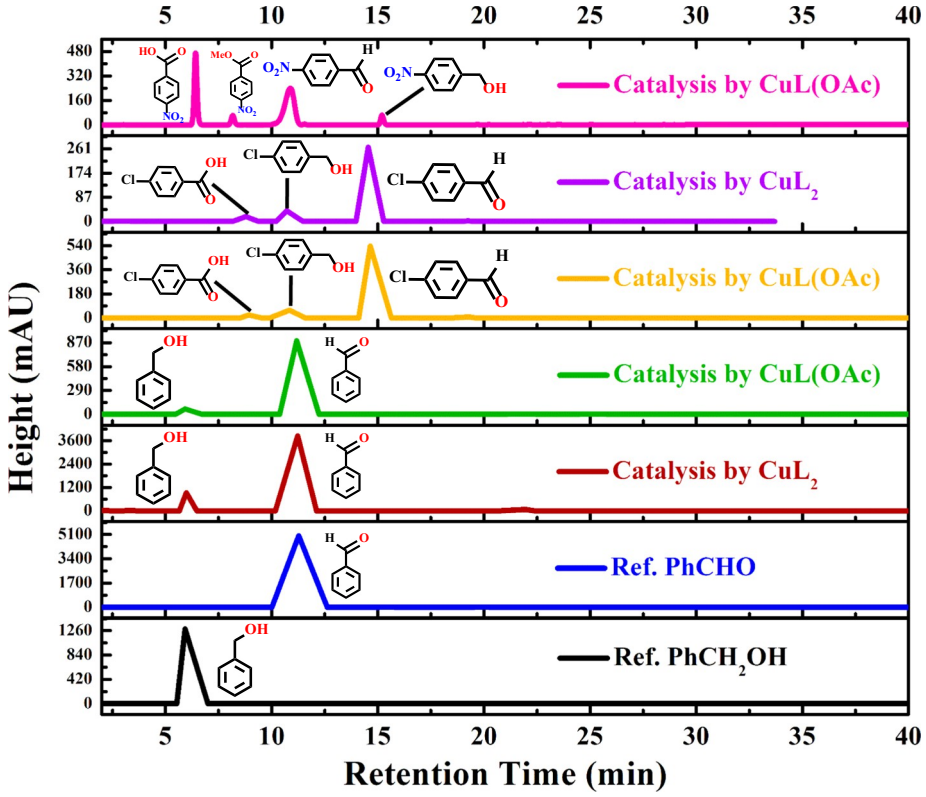

Fig. 4. HPLC interpretation of some oxidation reactions after catalysis ('Ref.' signifies the standard sample).

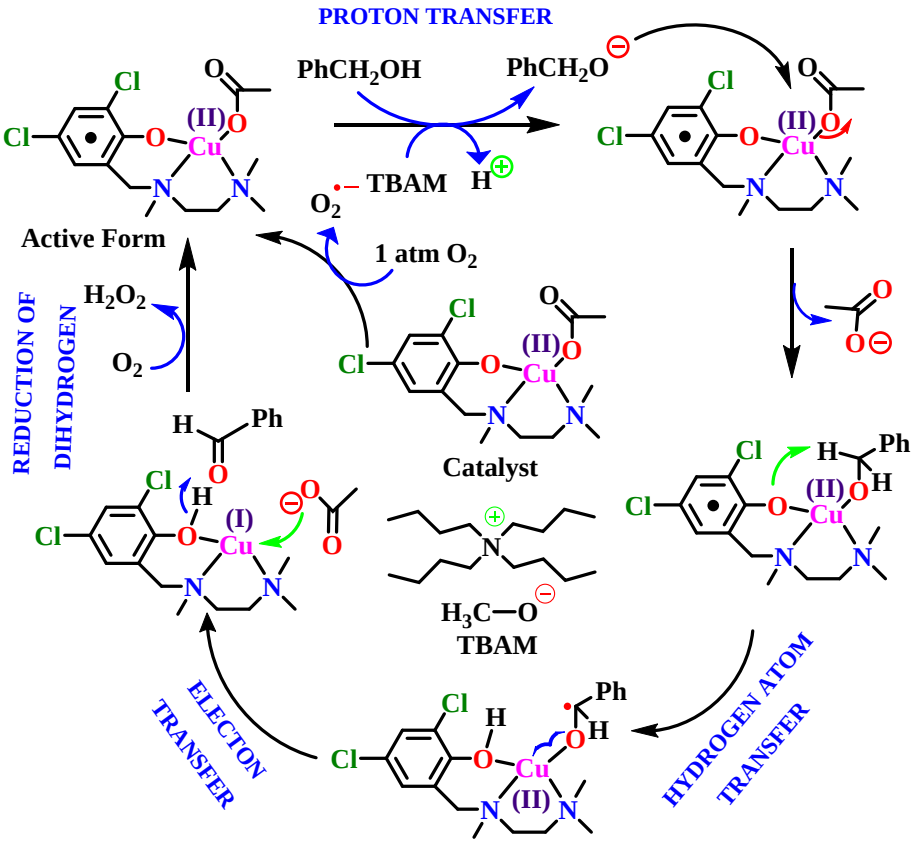

Scheme 2. Plausible mechanism for GOase mimicking catalysis by catalyst **1**.

Table 2
Summary of various kinetic parameters of catecholase like activity of catalyst **1**, and **2**. Compared with that of $\sim 1 \times 10^4\ h^{-1}$ of the most efficient catalyst reported till date [52] said by K. S. Banu et al. [53].

Complex/catalyst	Cat. conc. (in M)	Solvent	λ_{max} (nm)	V_{max} (M min^{-1})	K_m (M)	Standard error (%)	K_{cat}/TON (h^{-1})
1	4.0×10^{-4}	MeOH	440	1.3174	0.25306	1.8×10^{-2}	1.976×10^5
2	4.0×10^{-4}	MeOH	444	0.06928	0.04302	4.6×10^{-3}	1.039×10^4

obtained by dividing V_{max} value with the concentration of the corresponding complexes with respect to time. As summarized in Table 2, complex **1** and **2** is having the TON values of 1.976×10^5, and $1.039 \times 10^4\ h^{-1}$, respectively. These values are quite high in comparison to the previously reported analogous [49–51]. Moreover, the TON parameters of natural metalloenzymes have been compared with our laboratory synthesized complexes, and the corresponding values are summarized in Tables S6. Results suggest that catalyst **1** is more active over catalyst **2**. This might be due to the mono-ligand coordination, which is leading to the favorable substrate attachment as shown in Scheme 3.

3.4.2. Mechanism of action for COase like activity

To get an insight into the possible mechanism of COase like activity, complex **1** has been chosen due to its greater activity. We have explored the mechanism by ESI-mass spectrometry, as described as reported in earlier cases to investigate the probable complex-substrate intermediate formation during catalysis [54]. ESI-MS positive spectrum of a 1:100 equivalent ratio of catalyst **1** and 3,5-DTBC recorded after 5 min of mixing exhibits two major peaks at +, $m/z = 243.4$ and 463.6 respectively, along with two small peaks at 560.5 & 1143.9 (Scheme 3 and Fig. 5). The former two peaks correspond to the quinone-sodium aggregates $[(3,5\text{-DTBQ}) + Na]^+$ and $[(3,5\text{-DTBQ})_2 + Na]^+$ [55]. The later smaller peaks at 573.4 & 1143.9 might be attributed to the formation of monomeric and dimeric complex-substrate aggregate (Scheme 3) [53]. Notably, ESI-MS peak at 1143.9 is the signature of the original enzyme kinetic mechanism, where di-copper involves during COase mimicking catalysis. At the end of oxidation, the colour of the solution turned into brown, which gives a d-d transition band in UV–visible spectrum due to Cu(II) complex. Apart from that, the reduction of molecular oxygen took place resulting the formation of hydrogen peroxide in the reaction medium, which has been be elaborated further.

3.4.3. Detection of hydrogen peroxide during GOase and COase catalysis

It is also important to note that, at the end of catalysis (GOase or COase mimicked) the dioxygen of atmosphere is reduced to H_2O_2. Hence, for the qualitative or quantitative detection of reduced product (s) (H_2O_2 or H_2O), evolved during both catalytic reactions, a modified iodometric method was successfully employed [23,56]. Though, H_2O_2 can be determined amperometrically by direct oxidation or by reduction of mediators but we have followed a simple electronic spectroscopy for the detection [57]. The duration of collecting the catalytic mixture for GOase as well as COase mimicking catalysis were 12 h and 1 h, respectively.

Reaction mixtures for the determination of hydrogen peroxide were prepared as per method described in our previous literature [25]. It

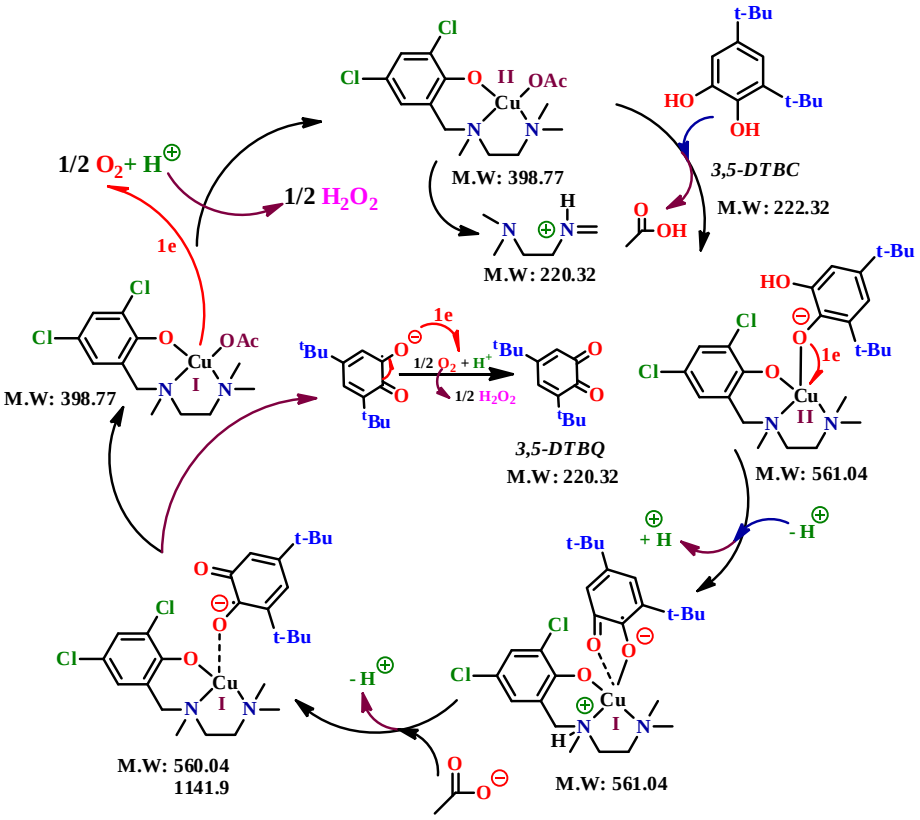

Scheme 3. Probable catalytic cycle of oxidation of 3,5-DTBC by complex **1**. Calculated mass of intermediates and product(s) are given in Fig. 5.

describes that after completion of kinetic experiments, an equal volume of water (say 10 mL) was added to the reaction mixture, and oxidized products (viz benzaldehyde or quinone) were extracted with 3 × 10 mL dichloromethane. After that, the aqueous layer was acidified with H_2SO_4 (5.0×10^{-3} mol L^{-1}) to pH ~ 2 (checked by pH-meter) to stop further oxidation. Then 1 mL of a 10% aqueous solution of KI was poured into the mixture followed by the addition of 3 drops of a 3% solution of ammonium molybdate.

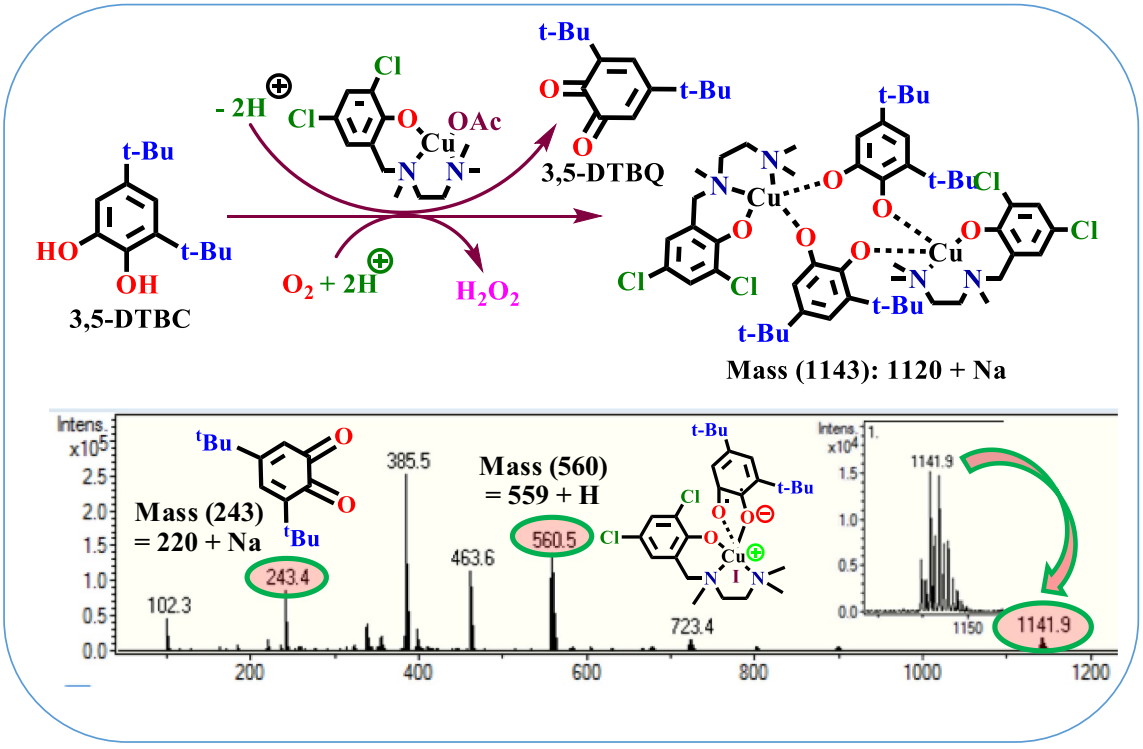

Fig. 5. Evidence of the formation of dimeric 'substrate-catalyst' bounded intermediate as described in Scheme 3.

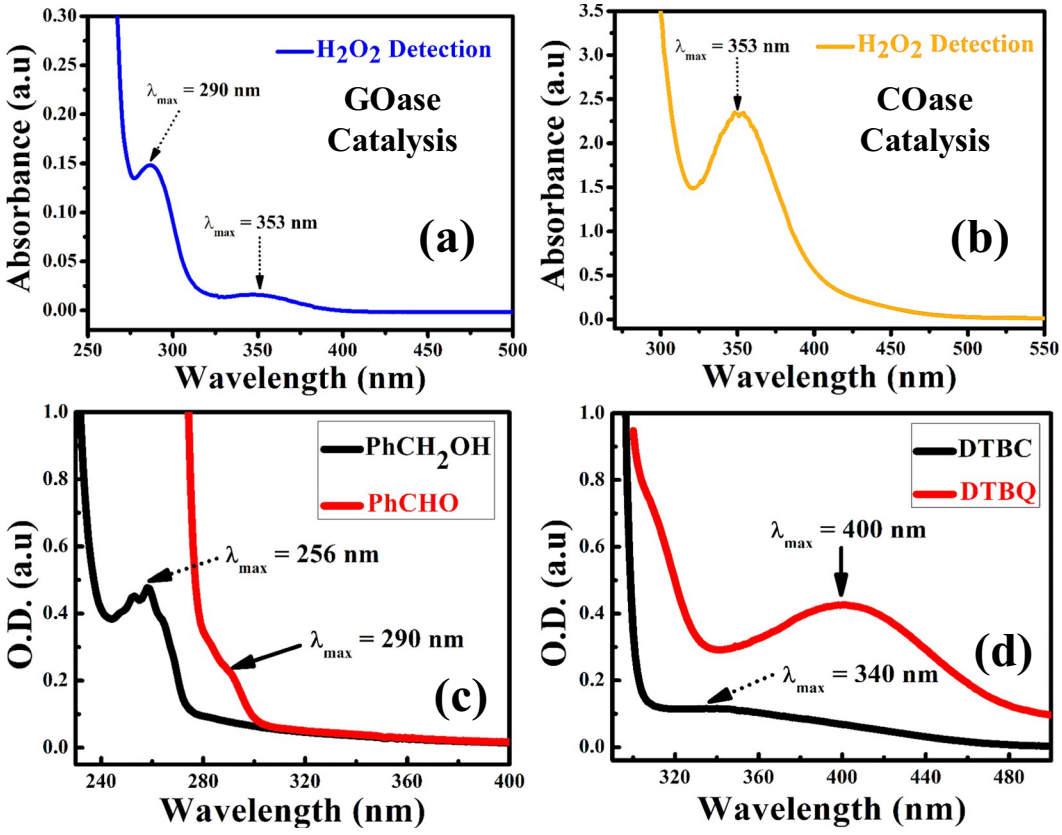

Fig. 6. Detection of hydrogen peroxide in the catalytic reaction: (a) formation of H_2O_2 (λ_{max} = 353 nm) as well as PhCHO (λ_{max} = 290 nm) during GOase catalysis, (b) H_2O_2 production during COase like activity monitored by UV–Vis spectra of the characteristic absorption band at λ_{max} = 353 nm, (c) and (d) represents the electronic spectra of the reference solution of substrates and products for GOase, and COase catalysis, respectively.

The I^- ions may further oxidized to I_2 in the presence of H_2O_2 as shown according to the iodometric reaction: $H_2O_2 + 2I^- + 2H^+ \rightarrow 2H_2O + I_2$ (aq.). An excess of iodide ions react with molecular iodine to produce highly stable tri-iodide ion (I_3^-) by following a reaction: I_2 (aq.) + $I^- \rightarrow I_3^-$. The rate of reaction is slow but increases with increasing concentrations of acid. However, upon addition of an ammonium molybdate solution the reaction can immediately cease. A characteristic I_3^- band at λ_{max} = 353 nm is depicted in the Fig. 6a–b. Fig. 6a represents the two kind of absorption maxima at 290 nm and 353 nm for GOase catalysis, respectively. Among which, the formation of benzaldehyde in the range of 290 nm is predominant which is a consequence of better solubility of benzaldehyde in aqueous medium [58]. Hence, all the above experiments hereby support the radical mechanism pathways for GOase or COase mimicking catalysis. Furthermore, the electronic spectra of the reference solution of substrates and products for GOase, and COase catalysis have been depicted in Fig. 6c–d.

4. Conclusions

In summary, the structure of Mannich base ligand and complex **2** were elucidated by single crystal X-ray crystallography, whereas geometry optimized model of complex **1** has been derived theoretically. Considering GOase liked catalysis, benzyl alcohol selectively produce only benzaldehyde by a percentage conversion of 93.43% and 92.80% in 8 h with respect to catalyst **1** and **2**, respectively. Furthermore, extremely high TON values of 1.976×10^5, and 1.039×10^4 per hour have been observed for complex **1** and **2**, respectively. Despite of being catalytically active, catalyst **1** follows a regular M-M kinetic mechanism, which resembles the mechanistic pathways of original enzyme. Apart from that, the labile nature of acetate group attached to the central copper atom of complex **1** might be responsible for the better catalytic activity for both the GOase and COase mimicking catalysis.

Acknowledgement

This work is supported by DST India under Indo-Portuguese joint collaborative project scheme (Grant Number INT/PORTUGAL/P-04/2013). We thank IIT Indore for proving the infrastructure, and financial support. The author is grateful to Dr. Auprba K. Das for his kind help in HPLC. We also express thanks to SIC, IIT Indore for the experimental facilities, and structure interpretation.

Appendix A. Supplementary data

CCDC **1882115** and **1455095** encompass the complementary crystallographic information for **HL**, and **2**, respectively. These information can be acquired free of charge via http://www.ccdc.cam.ac.uk/conts/retrieving.html, or from the Cambridge Crystallographic Data Center, 12 Union Road, Cambridge CB2 1EZ, UK; fax: (+44) 1223-336-033; or e-mail: deposit@ccdc.cam.ac.uk. Supplementary data to this article can be found online at https://doi.org/10.1016/j.jinorgbio.2019.03.023.

References

[1] S.K. Dey, A. Mukherjee, ChemCatChem 5 (2013) 3533–3537.
[2] K.D. Karlin, Science 261 (1993) 701.
[3] J.P. Klinman, Chem. Rev. 96 (1996) 2541–2562.
[4] R.A. Festa, D.J. Thiele, Current biology: CB 21 (2011) 877–883.
[5] E.I. Solomon, D.E. Heppner, E.M. Johnston, J.W. Ginsbach, J. Cirera, M. Qayyum, M.T. Kieber-Emmons, C.H. Kjaergaard, R.G. Hadt, L. Tian, Chem. Rev. 114 (2014) 3659–3853.
[6] M. Zhao, H.-B. Wang, L.-N. Ji, Z.-W. Mao, Chem. Soc. Rev. 42 (2013) 8360–8375.

[7] E.K. van den Beuken, B.L. Feringa, Tetrahedron 54 (1998) 12985–13011.
[8] J.W. Whittaker, Chem. Rev. 103 (2003) 2347–2364.
[9] M. Fontecave, J.-L. Pierre, Coord. Chem. Rev. 170 (1998) 125–140.
[10] W. Kaim, J. Rall, Angew. Chem. Int. Ed. Engl. 35 (1996) 43–60.
[11] F. Thomas, Eur. J. Inorg. Chem. 2007 (2007) 2379–2404.
[12] D. Yin, S. Urresti, M. Lafond, E.M. Johnston, F. Derikvand, L. Ciano, J.-G. Berrin, B. Henrissat, P.H. Walton, G.J. Davies, H. Brumer, Nat. Commun. 6 (2015) 10197–10210.
[13] E.I. Solomon, P. Chen, M. Metz, S.-K. Lee, A.E. Palmer, Angew. Chem. Int. Ed. 40 (2001) 4570–4590.
[14] Kirk-Othmer Encyclopedia of Chemical Technology, (2004).
[15] G. Gergely, US Patent, 4 (1984) 821.
[16] M. Dyrby, N. Westergaard, H. Stapelfeldt, Food Chem. 72 (2001) 431–437.
[17] D.M. Boghaei, M. Lashanizadegan, Synthesis and Reactivity in Inorganic and Metal-Organic Chemistry 30 (2000) 1393–1404.
[18] A. Philibert, F. Thomas, C. Philouze, S. Hamman, E. Saint-Aman, J.-L. Pierre, Chem. Eur. J. 9 (2003) 3803–3812.
[19] S. Gentil, D. Serre, C. Philouze, M. Holzinger, F. Thomas, A. Le Goff, Angew. Chem. Int. Ed. 55 (2016) 2517–2520.
[20] T. Klabunde, C. Eicken, J.C. Sacchettini, B. Krebs, Nat. Struct. Biol. 5 (1998) 1084.
[21] N. Hakulinen, C. Gasparetti, H. Kaljunen, K. Kruus, J. Rouvinen, JBIC Journal of Biological Inorganic Chemistry 18 (2013) 917–929.
[22] V.M. Virador, J.P. Reyes Grajeda, A. Blanco-Labra, E. Mendiola-Olaya, G.M. Smith, A. Moreno, J.R. Whitaker, J. Agric. Food Chem. 58 (2010) 1189–1201.
[23] M. Das, B. Kumar Kundu, R. Tiwari, P. Mandal, D. Nayak, R. Ganguly, S. Mukhopadhyay, Inorg. Chim. Acta 469 (2018) 111–122.
[24] L. Vámos-Vigyázó, N.F. Haard, C R C Critical Reviews in Food Science and Nutrition 15 (1981) 49–127.
[25] M. Das, R. Nasani, M. Saha, S.M. Mobin, S. Mukhopadhyay, Dalton Trans. 44 (2015) 2299–2310.
[26] M.R. Malachowski, M.G. Davidson, Inorg. Chim. Acta 162 (1989) 199–204.
[27] M. Merkel, N. Möller, M. Piacenza, S. Grimme, A. Rompel, B. Krebs, Chem. Eur. J. 11 (2005) 1201–1209.
[28] A.L. Abuhijleh, J. Inorg. Biochem. 55 (1994) 255–262.
[29] M.E. Kodadi, F. Malek, R. Touzani, A. Ramdani, Catal. Commun. 9 (2008) 966–969.
[30] P. Seth, L.K. Das, M.G.B. Drew, A. Ghosh, Eur. J. Inorg. Chem. 2012 (2012) 2232–2242.
[31] B. Sreenivasulu, M. Vetrichelvan, F. Zhao, S. Gao, J.J. Vittal, Eur. J. Inorg. Chem. 2005 (2005) 4635–4645.
[32] S.K. Dey, A. Mukherjee, New J. Chem. 38 (2014) 4985–4995.
[33] S. Biswas, S. Bhowmik, D.B. Rasale, A.K. Das, Macromol. Symp. 369 (2016) 108–113.
[34] C.K. Williams, L.E. Breyfogle, S.K. Choi, W. Nam, V.G. Young, M.A. Hillmyer, W.B. Tolman, J. Am. Chem. Soc. 125 (2003) 11350–11359.
[35] A.B.P. Lever, D. Ogden, Journal of the Chemical Society A: Inorganic, Physical, Theoretical (1967) 2041–2048.
[36] B. Kumar Kundu, V. Chhabra, N. Malviya, R. Ganguly, G.S. Mishra, S. Mukhopadhyay, Microporous Mesoporous Mater. 271 (2018) 100–117.
[37] B.K. Kundu, P. Mandal, B.G. Mukhopadhyay, R. Tiwari, D. Nayak, R. Ganguly, S. Mukhopadhyay, Sensors Actuators B Chem. 282 (2019) 347–358.
[38] H. Temel, S. İlhan, M. Aslano ğlu, A. Kiliçl, E. Taş, J. Chin. Chem. Soc. 53 (2006) 1027–1031.
[39] P. Guillo, O. Hamelin, F. Loiseau, J. Pécaut, S. Ménage, Dalton Trans. 39 (2010) 5650–5657.
[40] Y. Wang, J.L. DuBois, B. Hedman, K.O. Hodgson, T.D.P. Stack, Science 279 (1998) 537.
[41] D. Olea-Román, J.C. Villeda-García, R. Colorado-Peralta, A. Solano-Peralta, M. Sanchez, I.F. Hernández-Ahuactzi, S.E. Castillo-Blum, J. Mex. Chem. Soc. 57 (2013) 230–238.
[42] T. Steiner, Angew. Chem. Int. Ed. 41 (2002) 48–76.
[43] R. Taylor, O. Kennard, J. Am. Chem. Soc. 104 (1982) 5063–5070.
[44] S. Mukhopadhyay, B.K. Kundu, R. Singh, R. Tiwari, D. Nayak, New J. Chem. (2019), https://doi.org/10.1039/C9NJ00138G.
[45] F. Himo, L.A. Eriksson, F. Maseras, P.E. Siegbahn, J. Am. Chem. Soc. 122 (2000) 8031–8036.
[46] A. Martínez, I. Membrillo, V.M. Ugalde-Saldívar, L. Gasque, J. Phys. Chem. B 116 (2012) 8038–8044.
[47] E. Valero, R. Varón, F. García-Carmona, Biochem. J. 277 (1991) 869.
[48] A. Jana, N. Aliaga-Alcalde, E. Ruiz, S. Mohanta, Inorg. Chem. 52 (2013) 7732–7746.
[49] M. Saha, M. Das, R. Nasani, I. Choudhuri, M. Yousufuddin, H.P. Nayek, M.M. Shaikh, B. Pathak, S. Mukhopadhyay, Dalton Trans. 44 (2015) 20154–20167.
[50] J. Kaizer, G. Baráth, R. Csonka, G. Speier, L. Korecz, A. Rockenbauer, L. Párkányi, J. Inorg. Biochem. 102 (2008) 773–780.
[51] A. Neves, L.M. Rossi, A.J. Bortoluzzi, B. Szpoganicz, C. Wiezbicki, E. Schwingel, W. Haase, S. Ostrovsky, Inorg. Chem. 41 (2002) 1788–1794.
[52] R. Wegner, M. Gottschaldt, W. Poppitz, E.-G. Jäger, D. Klemm, J. Mol. Catal. A Chem. 201 (2003) 93–118.
[53] K.S. Banu, T. Chattopadhyay, A. Banerjee, S. Bhattacharya, E. Suresh, M. Nethaji, E. Zangrando, D. Das, Inorg. Chem. 47 (2008) 7083–7093.
[54] T. Chattopadhyay, M. Mukherjee, A. Mondal, P. Maiti, A. Banerjee, K.S. Banu, S. Bhattacharya, B. Roy, D. Chattopadhyay, T.K. Mondal, Inorg. Chem. 49 (2010) 3121–3129.
[55] S. Sarkar, S. Majumder, S. Sasmal, L. Carrella, E. Rentschler, S. Mohanta, Polyhedron 50 (2013) 270–282.
[56] J. Ackermann, F. Meyer, E. Kaifer, H. Pritzkow, Chem. Eur. J. 8 (2002) 247–258.
[57] H. Lundbck, B. Olsson, Anal. Lett. 18 (1985) 871–889.
[58] R.M. Stephenson, J. Chem. Eng. Data 38 (1993) 630–633.